Journal of Applied Geophysics 98 (2013) 100–112

Contents lists available at ScienceDirect

Journal of Applied Geophysics

journal homepage: www.elsevier.com/locate/jappgeo

Assessment of an ancient bridge combining geophysical and advanced photogrammetric methods: Application to the Pont De Coq, France

Cyrille Fauchard [a,*], Raphaël Antoine [a], Frédéric Bretar [a], Julien Lacogne [b], Yannick Fargier [c], Cindy Maisonnave [a], Vincent Guilbert [a], Pierre Marjerie [d], Paul-Franck Thérain [e], Jean-Paul Dupont [f], Marc Pierrot-Deseilligny [g]

[a] Centre d'Études Techniques de l'Équipement - Normandie Centre, ERA23, Université de Rouen, 10 chemin de la Poudrière, CS 90245, 76121 Le Grand Quevilly, France
[b] Centre d'Études Techniques de l'Équipement - Normandie Centre, DADT, Université de Rouen, 10 chemin de la Poudrière, CS 90245, 76121 Le Grand Quevilly, France
[c] Centre d'Études Techniques de l'Équipement - Normandie Centre, ERA44, 11 rue Laplace, CS 2912, 41029 Blois France
[d] Laboratoire ECODIV, Institut de Recherche et d'Enseignement en Sciences de l'Environnement, Université de Rouen, Place Emile Blondel, F-76821 Mont Saint Aignan Cedex, France
[e] Direction Régionale des Affaires Culturelles - Haute Normandie, Conservation Régionale des Monuments Historiques, 7 Place de la Madeleine, 76000 Rouen, France
[f] Laboratoire de Morphodynamique Continentale et Côtière, UMR 6143-CNRS, Université de Rouen, Place Emile Blondel, F-76821 Mont Saint Aignan Cedex, France
[g] École Nationale des Sciences Géographiques, 6 et 8 Avenue Blaise Pascal, Cité Descartes, Champs-sur-Marne, 77455 Marne la Vallée, Cedex 2, France

ARTICLE INFO

Article history:
Received 4 February 2013
Accepted 8 August 2013
Available online 26 August 2013

Keywords:
Arch bridge
Historical heritage
Ground penetrating radar
Electrical resistivity tomography
Photogrammetry

ABSTRACT

A high resolution geophysical survey was carried out on the Pont De Coq, a medieval stone arch bridge located in Normandy (France) in 2011 and 2012. Two complementary methods are used: Electrical Resistivity Tomography (ERT) and Ground PenetratingRadar (GPR). They allow to evaluate the structural state of the bridge and to characterize the subsurface around and beneath the bridge. An excellent correlation is obtained between the geophysical methods and the geological data obtained around the bridge. In order to improve the restitution of the geophysical data, an advanced photogrammetric method is performed, providing a high resolution 3D Digital Terrain Model (DTM) of the Pont de Coq. The advanced photogrammetry enhances the presentation of the GPR and ERT data. This approach is an easy-to-use, rapid and cost-effective tool for stakeholders. Finally, it is a promising and original method for improved interpretations of future geophysical surveys.

1. Introduction

In the last decades, public institutions have shown an increased interest in heritage conservation and monuments protection. For that purpose, geophysical methods have been used for 20 years as powerful tools to assist in the curation of buildings (Colla et al., 1997; McCann and Forde, 2001; Nuzzo et al., 2010; Orbán and Gutermann, 2009; Orbán et al., 2008; Ranalli et al., 2004).

Bridges exhibit complex structures (Boothby et al., 1998), built in various geological conditions. This characteristic makes the combination of geophysical methods necessary to obtain a meaningful model of the internal structure of such constructions and their environment. For instance, Flint et al. (1999) used the Electric Resistivity Tomography (ERT), the Seismic and the Ground Penetrating Radar (GPR) methods to observe masonry structures. GPR and infrared thermography were performed by Hing and Halabe (2010) to detect water infiltration and defects at the surface at the surface deck of a Glass-Fiber-Reinforced Polymer bridge. On masonry bridges, the GPR is one of the most used tool, due its high practicality in the field (Hugenschmidt and Mastrangelo, 2006; Solla et al., 2010, 2011a,b). Indeed, it can be applied on the different parts of the bridge (deck, wingwalls, sprandel walls, barrel) and provides a quick observation of potential disorders (voids, roots, water infiltration, etc.) within the bridge.

The first objective of this paper is to investigate the internal structure of a small masonry arch bridge called "Pont de Coq" crossing the Epte river located in Normandy, France. This 400 year-old bridge has been severely damaged by the vegetation during several tens of years and will be subject to a complete rehabilitation in the near future. Thus, the small dimensions of the structure (a few meters) make the use of the GPR clearly suitable for a preliminary characterization of the extent of the internal disorders.

The second objective of this work is the determination of the nature of the soil around the river and under the bridge. In particular, the characterization of the foundations lying beneath the abutments is critical, because it will strongly constrain the rehabilitation stages. In such an alluvial context, the ERT and GPR methods are suitable for a rapid imaging of the shallow subsurface (Doetsch et al., 2012; Ercoli et al., 2012; Gourry et al., 2003). We performed several GPR and ERT profiles along the road crossing the bridge, as well as in the transverse direction to the structure. GPR observations were also made along the arch barrel of the bridge. Finally, the subsurface of the two banks of the river near

* Corresponding author. Tel.: +33 235689295; fax: +33 235688188.
E-mail address: cyrille.fauchard@developpement-durable.gouv.fr (C. Fauchard).

0926-9851/$ – see front matter © 2013 Elsevier B.V. All rights reserved.
http://dx.doi.org/10.1016/j.jappgeo.2013.08.009

the bridge was observed using the ERT method. The geophysical measurements are compared with the sedimentary logs obtained from two boreholes drilled around the bridge.

The photogrammetric method is a technique allowing the three-dimensional (3D) reconstruction of an object from photos. Recently, techniques based on close-range stereophotogrammetry have proved their capacity to extract DTMs with submillimeter accuracies (Chandler et al., 2005). Such DTMs have the advantage of providing a large number of profiles over large areas in one measurement only. For instance, such tools have been successfully used with geophysical methods for the structural assessment of stone arch bridges (Arias et al., 2007; Lubowiecka et al., 2011; Solla et al., 2012). Despite impressive results, they require careful positioning and orientation of the cameras with respect to the surface, the use of bulky poles and vertical calibration to minimize perspective distortion due to the focal lens of the camera. There are several commercial and open source software package like Photosynth (Microsoft Live Labs/University of Washington) or Photomodeller Pro (Eos Systems Inc.) to generate 3D models of the photographed object. Moreover, they lack mathematical rigor in the formulation of the equations which leads to low accuracy for scientific application. Geophysicists and civil engineers increasingly need affordable, light but also accurate tools to study the subsurface or to survey buildings (Pierrot Deseilligny and Clery, 2011). As a summary, most of these techniques are difficult to use and none of them is fully satisfactory in terms of costs, applicability or spatial sampling. Recently, substantial progress has been made in the generation of DTMs, using photographic images taken by off-the-shelf digital cameras positioned at different locations around the target with a resolution ranging from millimeters to a few centimeters. For the first time, this article presents a rapid and cost-effective photogrammetric method described in Bretar et al. (2013) to improve the 3D presentation of geophysical data.

In Section 2, the historical context of the Pont de Coq and the geology of the region are presented. Section 3 is dedicated to the description of the geological data obtained at the local scale by the boreholes performed close to the bridge. Then, we present our geophysical data: the GPR measurements carried out on the bridge, in particular on the deck and the arch barrel are discussed in Section 4. This part is followed by the characterization of the surroundings of the structure by GPR and ERT (Section 5). Finally, a high resolution photogrammetric DTM of the Pont de Coq integrating the GPR and ERT data is presented in Section 6.

2. Study context

2.1. Historical context and location of the Pont de Coq

The Pont De Coq is an arch bridge located on an ancient royal road connecting Dieppe to Paris, between the Menerval and Saumont-La-Poterie towns (Fig. 1). It spans the Epte river, a 113 km long tributary of the Seine river. The bridge is thought to have been built at the beginning of the XVIIth century. The structure was preserved from wars, but it was progressively abandoned by the authorities during the last centuries, due to new roads and a railway constructions. Re-discovered in 2010, the Pont de Coq is now registered as an historical monument by the French Authorities and is restored by a non-profit organization (ASPC, Association pour la Sauvegarde du Pont de Coq).

In 2010, the first in-situ visits revealed several damages at the Pont De Coq. The wingwalls (upstream north wall and both downstream walls) are skewed and some stones have disappeared. The upstream south wingwall has been destroyed by a tree's root network (shown in Fig. 2). The roots also extend within the backfill material at the top of the abutment and under the roadway, which is paved with limestone stones perfectly jointed and overlaying a compacted silty layer. The road surface is regular with minor local deformations, probably due to the root network development into the silty layer and the backfill material. The voussoirs are joined with thin mortar and perfectly dressed and shaped. The intrados and extrados follow a semicircular arch ring. It can be noted that the voussoirs are shaped in polygonal extrados. This roman construction technique appears in the French civil engineering at the beginning of the Renaissance (XVIIth century). Despite the apparent bad condition of the bridge, only one crack is visible on the barrel surface at the downstream side. The arch is perfectly semicircular and the mechanical conditions of the bridge allow a low traffic of vehicles. An inspection at the bottom of the abutments also assumes the presence of driven wood piles anchoring the bridge in an unidentified layer.

2.2. Geological background

The Pont De Coq is built in the alluvial plain of the Epte River. The alluvions of the river at the regional scale are essentially composed of silty sand (Blondeau et al., 1979) that lays either on Quaternary colluvium or Upper Jurassic layers. The deposits are distributed as follows (Fig. 3):

- Quaternary limestone colluvium resulting from the erosion of Middle Portlandian deposits (clay, marl and limestone) or Middle to Upper Portlandian sediments (clay, sand and sandstone);
- An Upper Portlandian (Upper Jurassic) formation exhibiting sandy clay at the base of the layer and fine ferruginous sand at the top;
- A Middle Portlandian (Upper Jurassic) formation composed of i) a gray/blue clay layer at the bottom, ii) alternation of sand and sandstone layers at the middle and iii) marly limestone deposits at the top;
- A Lower Portlandian (Upper Jurassic) formation composed of an alternation of clear lithographic limestone and gray marl;
- A Kimmeridgian (Upper Jurassic) formation mainly composed of gray and/or blue clay.

3. Geological drilling

A complete study of the local geology and the geomorphology of the alluvial plain at the vicinities of the Pont de Coq has been achieved by Maisonnave (2012). In order to determine the nature of the subsurface at the local scale around the bridge, two boreholes were drilled near the Pont De Coq (numbered 1 and 2, in Fig. 5a) at the south and the north sides of the bridge (Fig. 5a and b). This geotechnical investigation was performed using a helical auger lent by the University of Rouen (Fig. 4). This method allows a good preservation of the lithological sequences. However, some sedimentary structures such as laminations or sorting may be partially destroyed when the soil is not cohesive enough. Thus, we only focus on the lithological nature of the observed sediments. The geological log of the first borehole (Fig. 5a) exhibits a silty layer road surface between 0 and about 40 cm depth, followed by a clayey layer between 40 cm and 1 m depth and a sandy layer with pebbles between 1 m and 2.5 m depth. Under this limit, the observed material is composed of Middle Portlandian clay. The geological log of the second borehole shows a similar layering, with a drilling refusal at 3 m depth.

The borehole logging provides a detailed description of the geology at the local scale around the bridge. However, such operation remains semi-destructive and punctual. In the next sections, we use the GPR and ERT geophysical methods to characterize the internal structure of the bridge (deck and arch barrel, Section 4) and the subsurface on which it was built (Section 5) without any destructive operation.

4. Non destructive assessment of the Pont De Coq masonry with GPR

For all geophysical surveys in this study, we define both the letters z and x respectively as the depth and the distance along the geophysical profile at which is observed an anomalie. In this section, we present the GPR survey carried out on the deck and the arch barrel of the Pont de Coq. Our objective is to determine whether voids, deformations or a tree's root network are present within the structure. Four longitunal

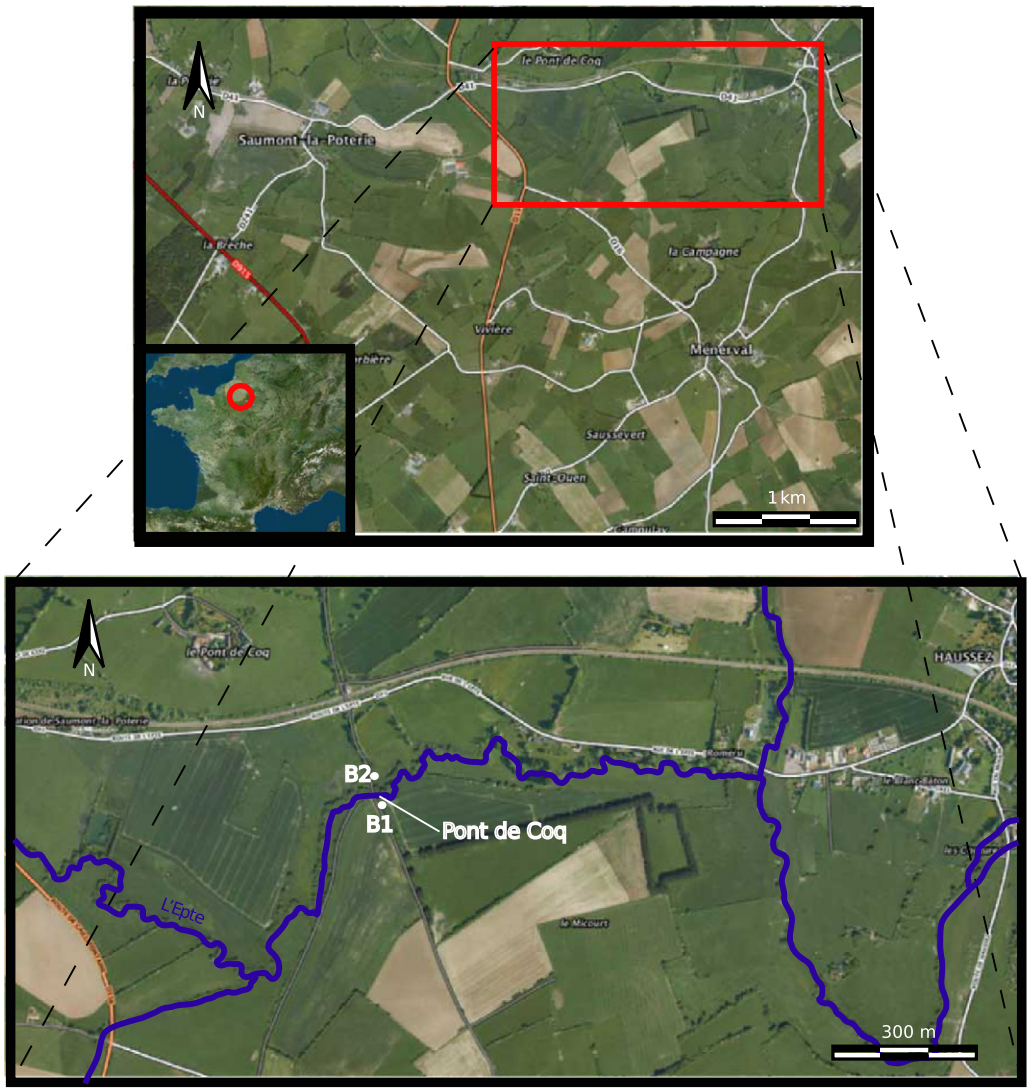

Fig. 1. Location of the Pont de Coq in the Normandy Region.

and eleven transversal profiles (1 m and 0.5 m spacing, respectively) were performed on the bridge deck using a 400 MHz bowtie antenna (Section 4.2). Five transversal and twelve radial profiles (1 m and 0.25 m spacing, respectively) were carried out on the surface arch barrel with a 1.5 GHz bowtie antenna (Section 4.3).

4.1. Processing of the GPR survey

A basic processing has been implemented on the GPR data. For this purpose, we used the Reflex™ Software (Sandmeier, 2004). The processing consists of a static correction in order to compensate the time

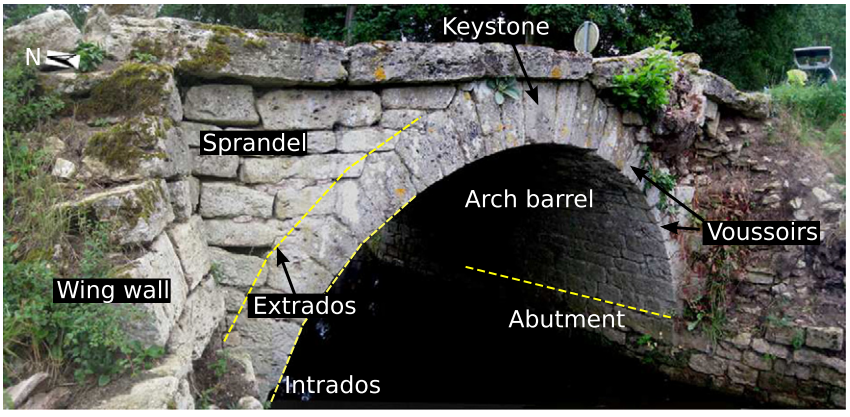

Fig. 2. Photography and description of The Pont De Coq (upstream view).

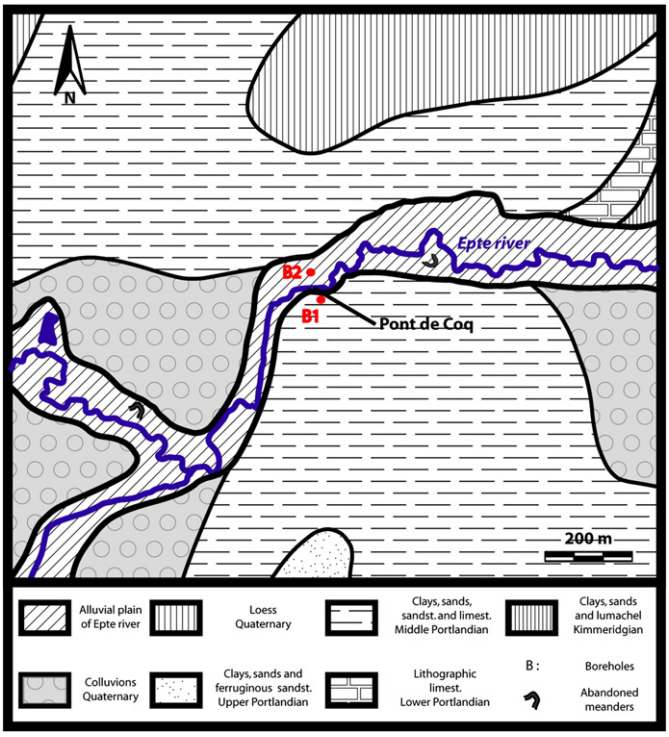

Fig. 3. Simplified geological map at the Pont De Coq.

delay of the first arrival and set the time 0 at the surface level of the investigated part of the bridge. Then, the gain function applied during the survey is removed. A background removal filter is applied to get rid of the noise due to the reflection of the waves within the antennas well as the antenna/ground interface. The signal is enhanced by an automatic gain control (AGC) function. Considering an average velocity of 0.1 m/ns (i.e. a relative dielectric permittivity of 9 for a multilayered media composed of limestone stones and silty material), the two-way travel time is converted to depth. A house code was developed with the Matlab™ Software to restitute the GPR survey carried out on the arch barrel (radial profiles). The GPR was able to penetrate entirely into the bridge, and down to 3 meters into the soil surrounding the structure at both riverbanks.

Fig. 4. Photography of the helical auger used for the geotechnical investigation.

4.2. GPR survey on the bridge deck

Fig. 6 shows the four profiles performed in the longitudinal direction (north) on the deck (C141 to C144 profiles). The vault is clearly identified by hyperbolas at mid-distance on the profiles. The C144 profile shows that the road is made of a first paved layer with limestone blocks of about z = 0.25 m thick (first white dashed line on C141 profile, Fig. 6). It is followed by a silty layer of about 0.3 m thick compacted and implemented on the external arch barrel (second white dashed line on the C144 profile). The same remarks can be formulated for the three other profiles. From the C141 to the C144 profiles, at about x = 6 m, little hyperbolas are observed across the bridge under the paved surface at about z = 0.3 m (two white dashed line crossing the 4 profiles). We argue that these hyperbolas are associated with the tree's root network. This hypothesis is supported by the observation of the roots on the south sprandel wall, as shown in Fig. 2. On the north side, defects (blue dashed rectangles, Fig. 6), similar to weathered zones or delamination are visible between z = 0.25 m to z = 0.5 m under the paved surface on the four profiles. The other parts of the bridge seem to be homogeneous.

The 400 MHz GPR transverse profiles on the deck are displayed in Fig. 7. The previous hyperbolas associated to the roots at the south side are retrieved on the C146, C147 and C155 profiles around 1 m long, between z = 0.2 m and z = 0.5 m. The weathered areas or delaminations at the south side are observed on the C154 and C155 profiles between x = 4 and x = 5 m (white dashed ellipses, Fig. 7) at z = 0.5 m. The white dashed lines on the C145 and C153 to C155 profiles underline the contact layer between the deck surface (limestone stones) and the silty material. The top of the arch barrel is underlined by the blue dashed line drawn on the C148 to C151 profiles. On these profiles, its depth varies because of the cylindrical shape of the arch. Strong diffractions appear at both the beginning and the end of these profiles, corresponding to the vertical contact between the bridge and the air underneath the arch barrel.

4.3. GPR survey on the arch barrel

The arch barrel is a key structure to investigate. The visual inspection showed that the arch is in good condition, with a minor crack on the top of the vault at the east side. In this section, our objective is to detect potential disorders just behind the voussoirs.

Longitudinal profiles were performed on the arch barrel towards east (Fig. 8). As it is shown on all these profiles, the disorders appear between z = 0.2 m and z = 0.3 m and the GPR signal at this location is similar to a void signature. The strong anomalies on the two first profiles (Fig. 8a, b and c) reflect the contact between the stones and the backfill material, with the potential presence of a root network and some voids. The profile carried out on the keystone exhibits weaker reflections (Fig. 8c): such phenomenon may be explained by gravitational compaction and losses of porosity induced by the traffic. The road surface fits an irregular curve (white dashed line). This anomaly is explained by (1) the cambered surface of the road and (2) the varying velocity of electromagnetic waves in the deck, due to the heterogenous distribution of materials. In Fig. 8d, deeper and stronger anomalies are detected (two white dashed ellipses): first, between z = 0.4 m and z = 0.7 m and between x = 1 m and x = 2 m and second, between z = 0.4 m and z = 0.7 m and between x =

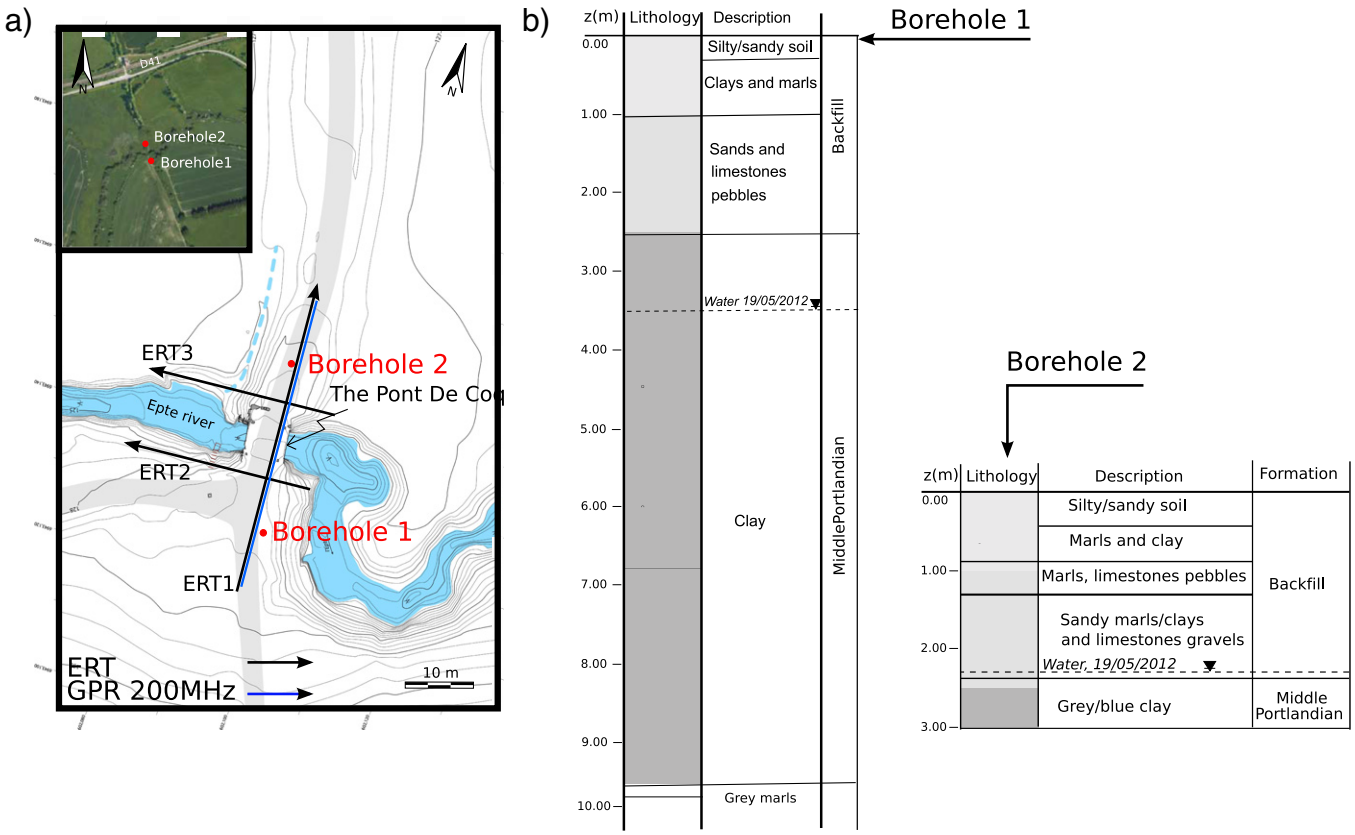

Fig. 5. a) Location of the geophysical profiles and the boreholes, b) geological logs of the two boreholes.

2.5 m and x = 3.2 m. These anomalies may be voids or weathered materials in the backfill. Some strong reflections observed between z = 0.2 m and z = 0.5 m and between x = 3 m and x = 6 m are correlated with a delamination between stones observed at the north feet abutment (Fig. 8e).

The radial profiles (three profiles shown in Fig. 9) were performed from south to north feet abutments. In this paragraph, the distance x refers to the south to north semi-perimeter of the arch. No defect seems to be present within the perfectly joined voussoirs (from z = 0.20 to 0.30 m). Local and shallow surface anomalies (Fig. 9b at x = 1.9 m and Fig. 9c at x = 3.6 m) reflect the bad contact between bowtie antenna and the voussoirs surface during the survey. The root network of an old tree present in the south sprandel wall (see Fig. 2) is probably detected: first, as shown in Fig. 9a, at x = 0.5 m and z = 0.3 m, and at

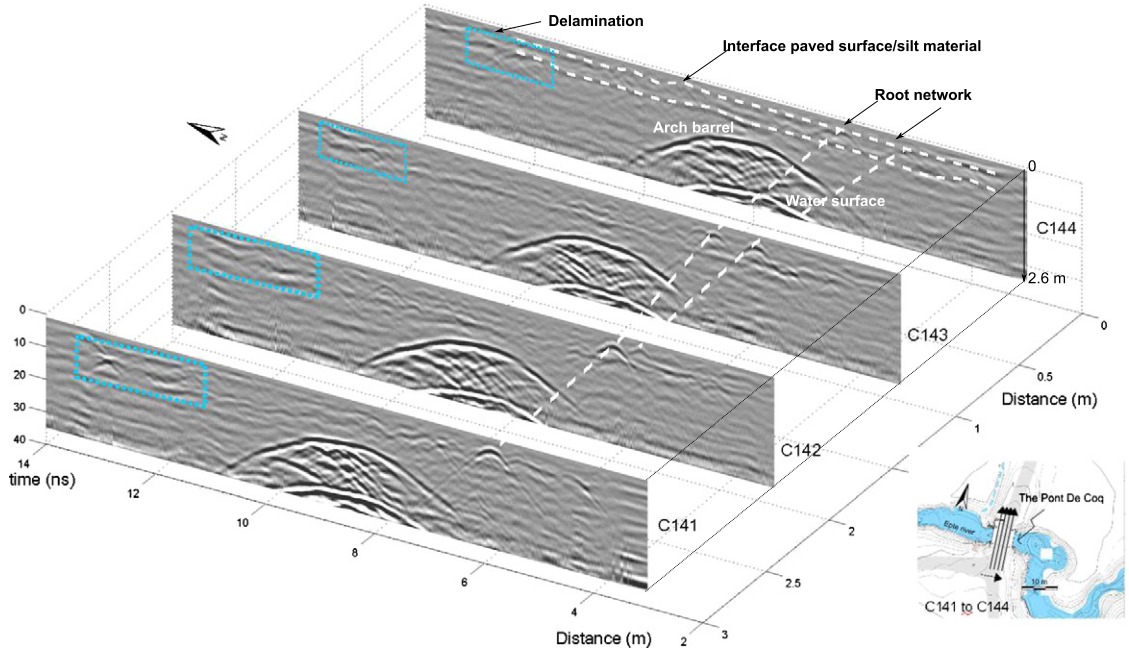

Fig. 6. 400 MHz GPR profiles performed on the bridge deck from south to north direction.

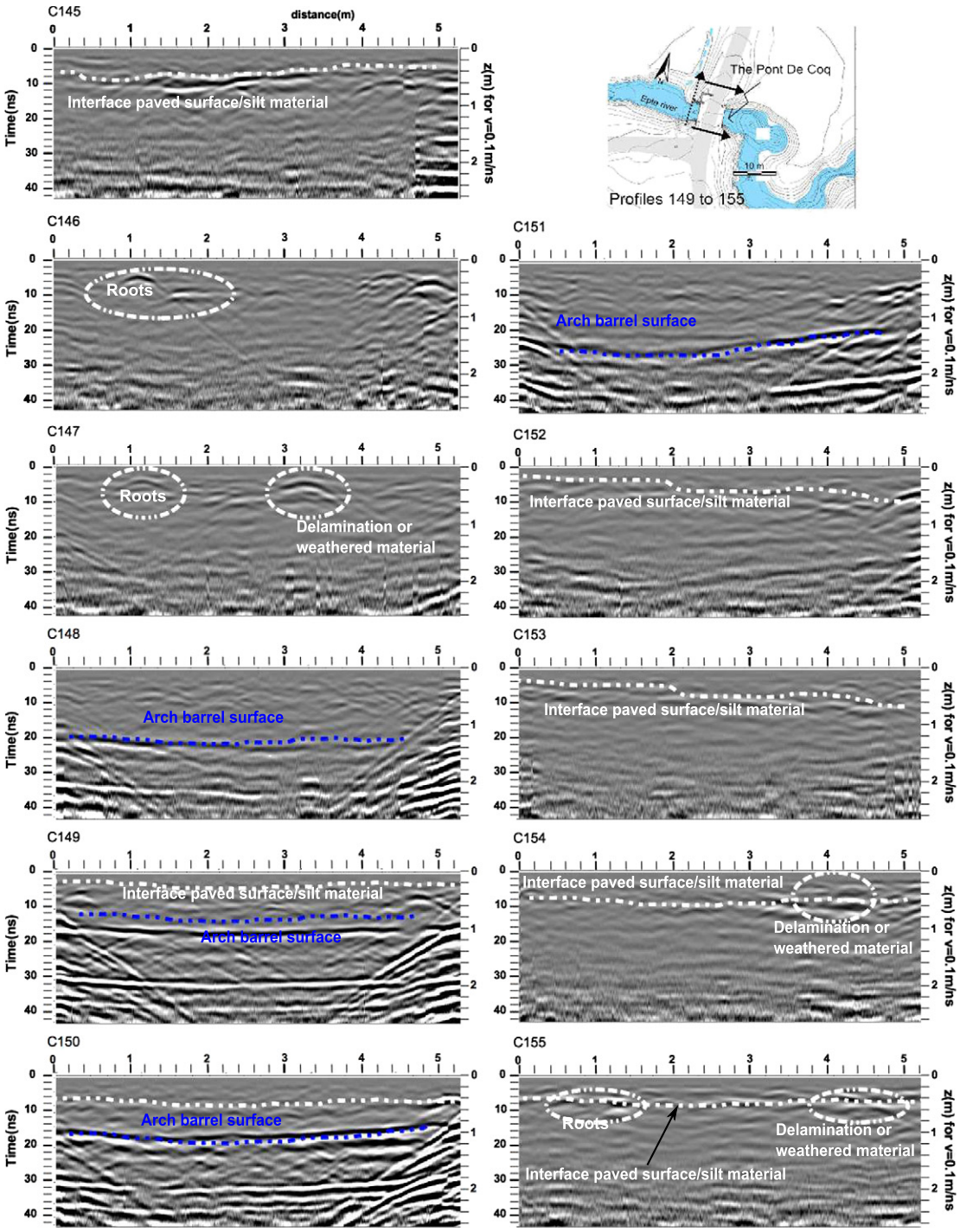

Fig. 7. 400 MHz GPR profiles performed on the bridge deck from west to east direction.

x = 1 m and z = 0.5 to 0.6 m and, second, as shown in Fig. 9c, at x = 0.5 m and z = 0.3 m, and at x = 1 m and z = 0.5 to 0.6 m. On the west profile, a defect (the road/air interface or a void under the paved surface) is detected at z = 2.2 m and z = 0.7 m. This anomaly appears on the east profile at x = 2.9 m at z = 0.7 m, where the survey line crosses the arch barrel keystones. However, it doesn't appear in the middle profile, where the backfill material is highly compacted and its thickness greater, as shown in Fig. 8c of the previous paragraph. The anomalies at z = 4.6 m and z = 0.5 m (Fig. 9b) may be voids in the backfill between the road and the abutments but they have not been compared with destructive testing for a more complete assessment.

In summary, the 400 MHz and 1.5 GHz GPR measurements carried out on the bridge deck and on the arch barrel, respectively, provide:

- The location of roots of trees inside the south abutment and under the paved surface;
- The location of both unknown anomalies inside the backfill material and weathered zones under the paved surface at the north side.

5. ERT and GPR surveys of the surroundings of the Pont de Coq

The objectives of this section are to characterize (1) the two riverbanks and (2) the way the road structure were implemented. We

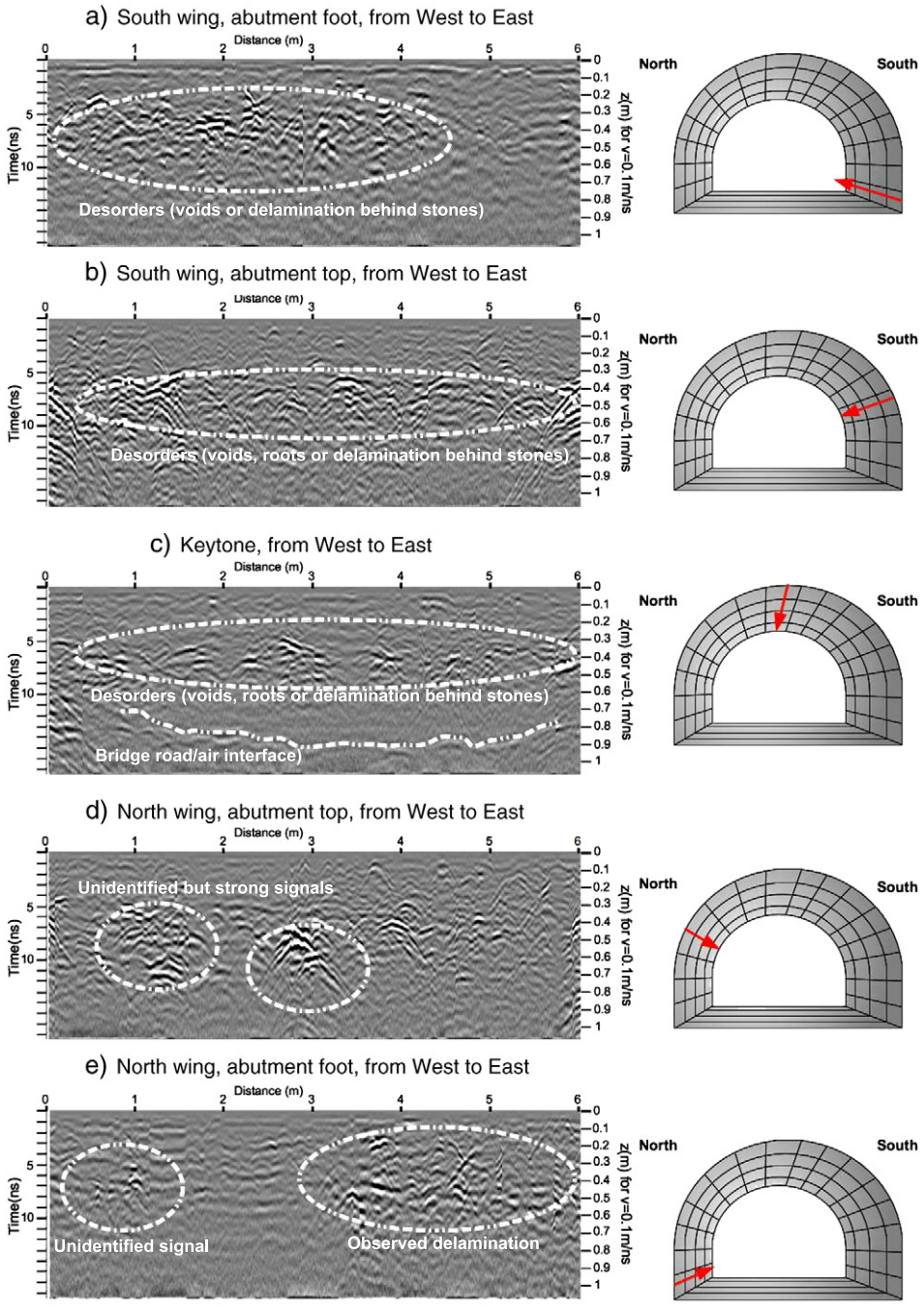

Fig. 8. 400 MHz GPR profiles performed on the arch barrel from west to east direction.

describe the processing of the ERT data in section (Section 5.1). The ERT models obtained on the two riverbanks are presented in section (Section 5.2). Finally, Section 5.3 presents the ERT model calculated along the road crossing the bridge. This last section leads to a first model of the bridge and its surroundings, taking into account both the previous data (geological study and geotechnical investigation) and a 200 MHz GPR survey made on the same location than the ERT survey.

5.1. Implementation and processing of the ERT survey

We aimed to explore an ancient road structure (depth and extension). For that purpose, an ERT configuration sensitive to vertical electric variation like the DD array (Locke, 2012) was appropriated. The method is efficient in mapping vertical structures (buried walls, dykes and cavities), but poor in mapping horizontal structures such as sedimentary layers. We used a Syscal Pro resistivimeter (Iris Instrument™) with a 48 electrodes DD array (23.5 length) and a 0.5 m spacing between the electrodes. Severe conditions are selected in order to (1) limit its noise sensitivity and (2) increase the imaging capability of the DD protocol. First, the electrodes were accurately positioned and a good contact between the ground and the electrodes was achieved. Second, in order to increase the data density, the dipole length a and the dipole separation factor n both vary from 1 to 7, leading to (1) 1047 quadripole measurements, (2) good measurements conditions (high quality factor) and (3) a limitation of the maximum geometrical factor. The DD array depth of investigation is usually underestimated by about 20% to 30% for the high n factor.

The inversion of the raw data was realized with the Res2Dinv™ software (Loke and Barker, 1996). The Jacobian matrix is inverted at each iteration and the data are corrected from the topography.

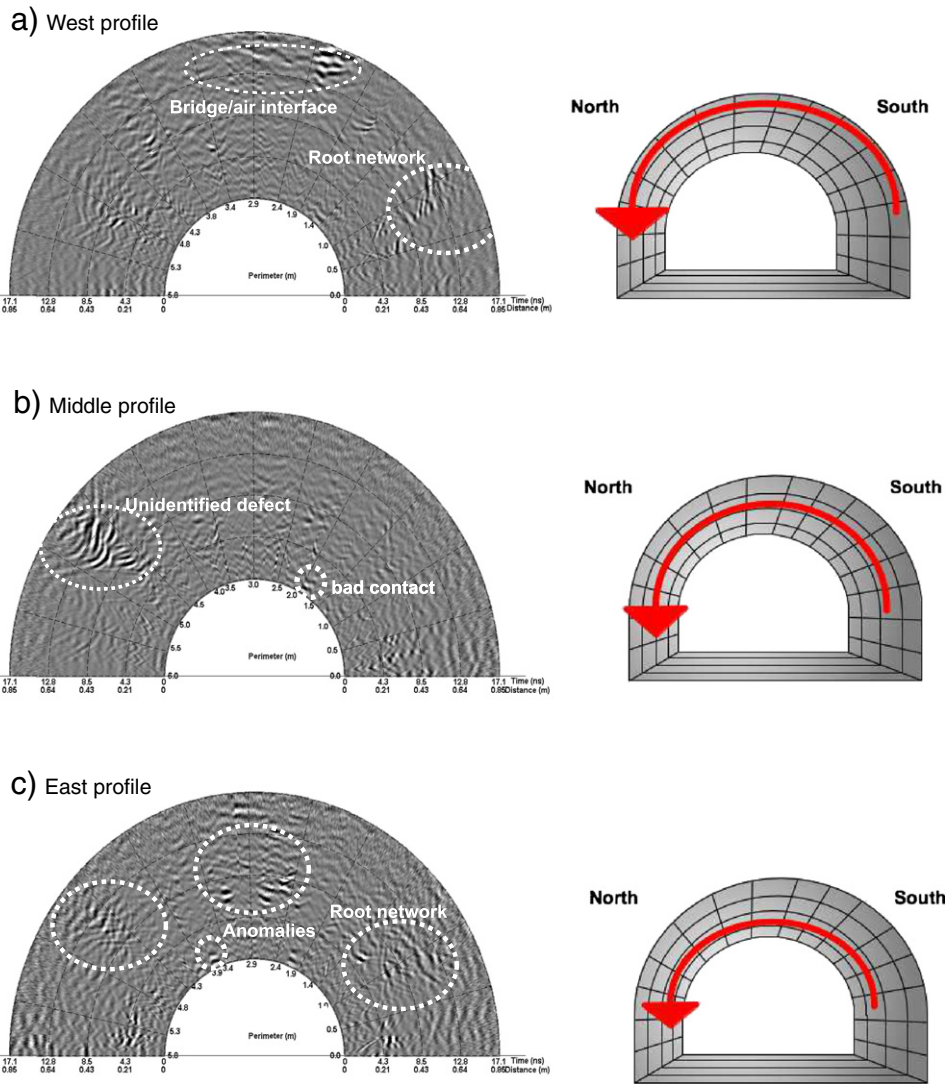

Fig. 9. 400 MHz GPR profiles performed on the arch barrel from south to north direction.

5.2. ERT on the two riverbanks

ERT measurements were performed on the two banks of the Epte river. The main objective of this section is to characterize the transition between the bridge and the riverbanks. The south and north profiles are shown in Figs. 10 (ERT2) and 11 (ERT3), respectively. The ERT2 profile shows that the clay layer is present at a shallow depth ($z = 2.5$ m) at the south side, and not detected at the north side. Fig. 12b, Section 5.3 also states that the clay layer is deeper at the north location. In fact, a longer profile or another ERT array such as Wenner Schlumberger or Pole-Pole at the north side should have been carried out in order to complete the description of the local geology. The ERT2 profile also

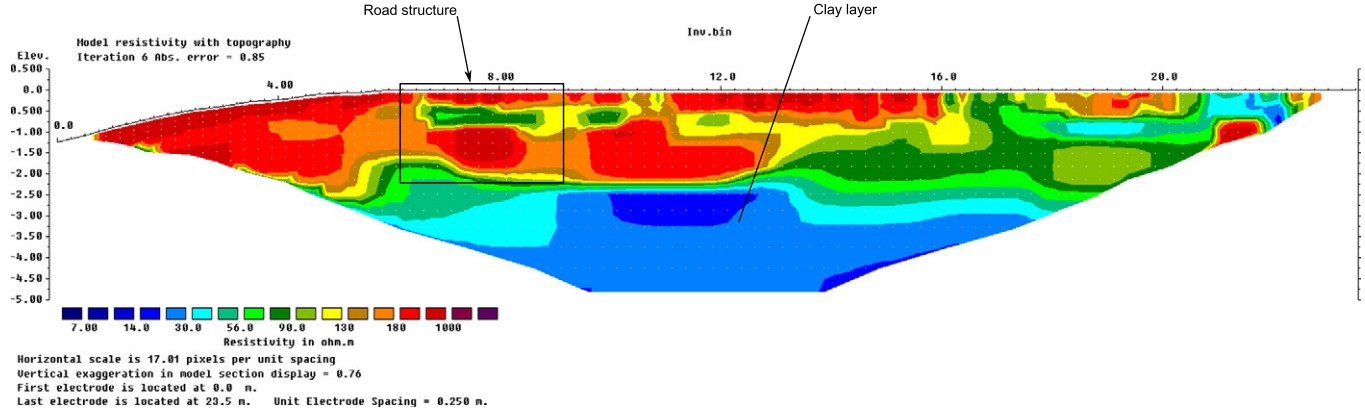

Fig. 10. Dipole–Dipole ERT2 profile performed on the south riverbank.

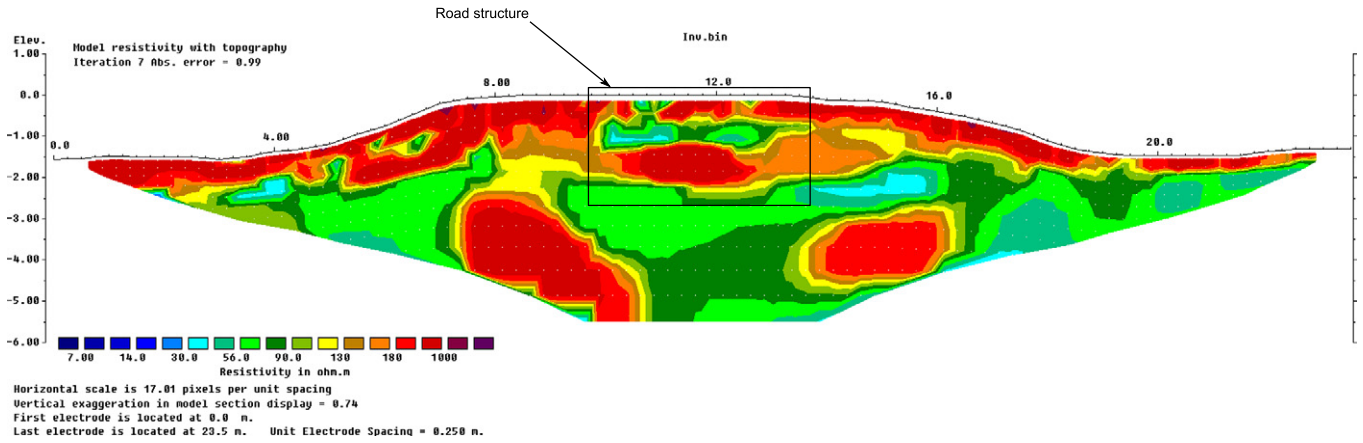

Fig. 11. Dipole–Dipole ERT3 profile performed on the north riverbank.

clearly shows the resistive road layers between x = 6 m and x = 9 m and extend to x = 14 m. Below x = 14 m, the structure of the riverbank is heterogeneous and its interpretation is not the objective of this work.

The ERT3 profile made at the north side of the bridge (Fig. 11) displays a resistive backfill material located at z = 2 m between x = 8 m and x = 13 m. It corresponds to the road base layer. The two resistive pockets between x = 8 m and x = 14 m length (at z = 2 m and z = 4 m, respectively) are not interpreted because they strongly depends on the array configuration.

In conclusion, these ERT measurements clearly identify the road base layer both inside the north and south riverbanks, and detect the clay layer at a shallow depth at the south side.

5.3. ERT along the road crossing the bridge

The last ERT profile (ERT1) was performed with a DD array configuration along the roadway crossing the bridge. In this case, 48 electrodes were used with a 1 m spacing. The DD inversion results are shown in Fig. 12b. A priori information was set to the inversion process in the Res2Dinv™ software: the vault was considered as a high resistive zone. Hence, it is detected between x = 22 m and x = 27 m and appears as highly resistive medium (void). On both riverbanks, the road layers and the bridge abutments are built with resistive materials in the first meter. On the south side, the pavement structure from x = 1 m to x = 10 m is quiet homogeneous in the first meter depth. The clayey materials clearly appear as very conductive materials (blue color,

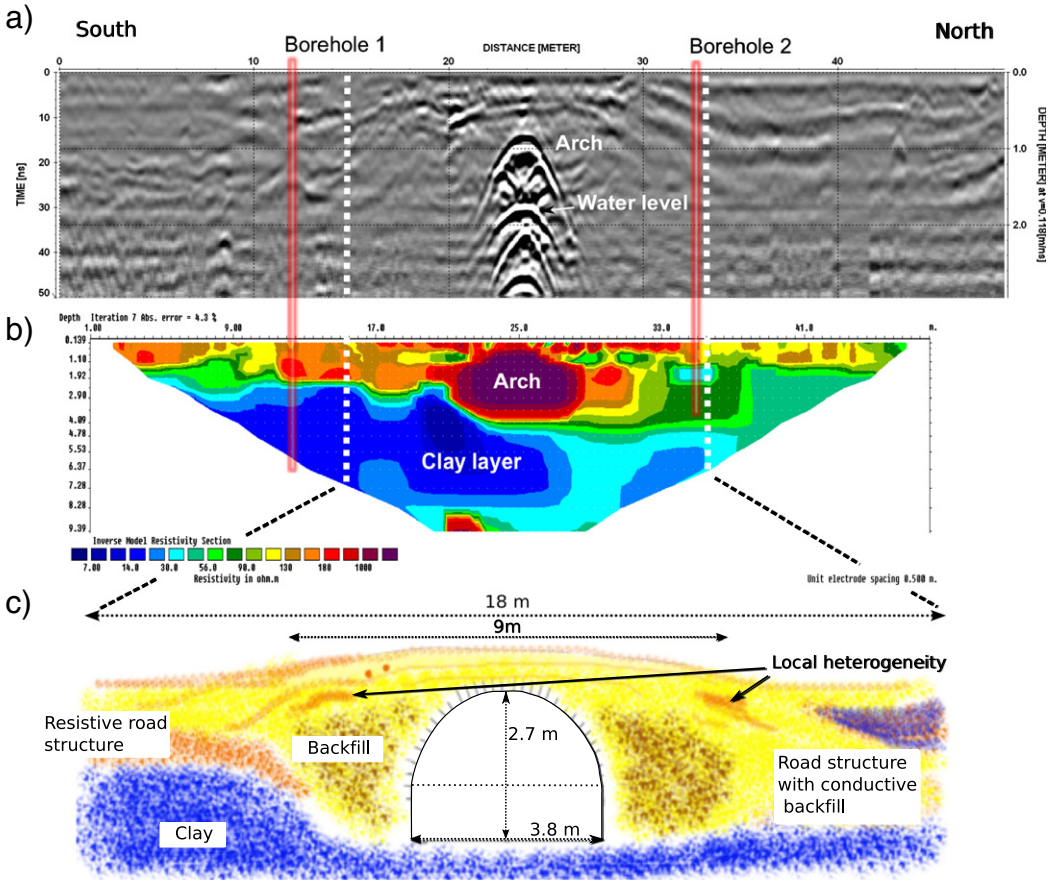

Fig. 12. a) 200 MHz GPR profile, b) ERT1 Dipole–Dipole profile, both performed on the roadway and c) subsurface model deduced from the geophysical measurements.

Fig. 13. Two images of the bridge acquired with different angles of view.

less than 20 Ω m). We note that the depth of this clayey layer in the ERT inversion results is located at a shallower depth ($z = 2$ m) than in the borehole logging because the DD array underestimates the depth of the structures.

On the north side, the basement is characterized by a resistive pocket (about 200 Ω m between $x = 26$ m and $x = 32$ m length) just after the abutment. It can be backfill materials implemented in order to make plane the roadway between the bridge deck and the north road. Then, from $x = 33$ m to the end of the profile, the pavement structure is thinner and the base course is filled with more conductive materials. The ERT measurements don't allow the detection of the expected and resistive limestone substratum (Middle Portlandian). The profile length is too short and the DD configuration is inappropriate for this detection.

A GPR profile was made on the roadway to complete the ERT survey. This method is usually suitable with a limited depth of penetration in alluvial context: the electromagnetic waves at GPR frequencies don't propagate in conductive matter. However, it can provide useful information for the imaging of both the road structure and the transitions between the bridge and the river sides. A longitunal measurement precisely located on the previous ERT1 profile was performed with a 200 MHz bowtie antenna. The B-scan (Fig. 12a) clearly shows the vault as a hyperbola (between $x = 22$ m and $x = 25$ m), corresponding to the classical response of a cylindrical object (the arch barrel) in GPR prospecting. Between these two positions, the following reflections are related to multiple travel paths between the arch barrel stones and the water surface. The previous ERT interpretation concerning the road structures (surface and base course) and the clay layer are well emphasized by the GPR survey. The electromagnetic waves easily propagate in the resistive layers (road base layer) and the clay acts as an absorbing matter.

In summary, the geophysical survey enables the following intermediate conclusion:

- The road base layer is well located inside both north and south riverbanks (Figs. 10 and 11);
- The clay layer is at a shallow depth at the south side (ERT2, Fig. 10 and ERT1, Fig. 12);
- The bridge piles under the abutments were probably driven in the alluvial Portlandian clay without being anchored to the Middle Portlandian limestone substratum. Nevertheless, the clay is a stable mechanical medium that has supported during centuries the Pond De Coq.

In order to help the stakeholder in the interpretation of the geophysical measurements, a simple model (Fig. 12c) is proposed. This interpretation is a first result that can be enhanced by a pseudo 3D view of the geophysical measurements integrated in a 3D model of the bridge, which is the main purpose of the following section.

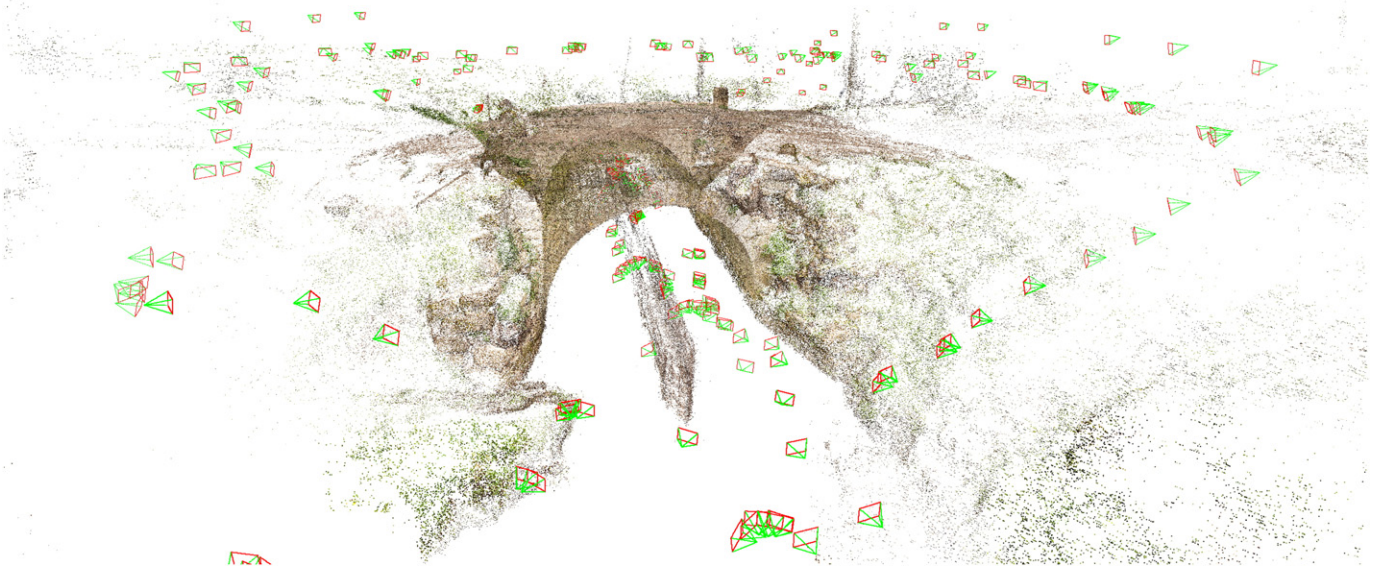

Fig. 14. 3D point cloud of the bridge. The pyramids represent the camera fields of view, as computed by the Apero module.

Fig. 15. Densified 3D model of the Pont de Coq.

6. Generation of a high resolution digital elevation model of the bridge with the photogrammetry method

In this section, we use a multi-view stereo software packages called Apero-MicMac (Aérotriangulation Photogrammétrique Expérimentale Relativement Opérationnelle Multi-Images Correspondances, Méthodes Automatiques de Corrélation) to generate a DTM of the Pont de Coq from photos acquired at arbitrary positions. Our geophysical data are then integrated within the obtained model.

Apero-MicMac uses a set of images and camera parameters (focal length and pixel size) to create a depth map of the scene, converted into a 3D point cloud. Detailed information on this tool is available at (http://www.micmac.ign.fr/). Apero-MicMac consists of three modules:

- The first module, a key step of unoriented image coregistration, selects all the pairs of images and searches those in which tie-points (vertex and corners of objects characterized by high gradients) are present. A Scale-Invariant Feature Transform (SIFT) is applied to extract local features in optical images (Lowe, 2004). The SIFT method is invariant to image scaling, translation and rotation, and partly invariant to illumination and 3D viewpoint changes. These properties make it a good candidate for analyzing relatively flat terrains such as bare soils.
- The second module, called Apero, automatically computes the relative orientation of the images. First, they are oriented one after the other relative to a master image. The order of priority is given by the number and distribution of the tie-points extracted by the first module. Then all initial orientations are iteratively adjusted at the same time. Other sources of information like GPS measurements, ground control points, reference objects, etc. may be used at this stage. The main challenge is to choose a good initial guess for the relative orientations. A poor estimate of this configuration is a common cause of failure. The way the data are acquired is therefore crucial: spending more time in the field during the experiment can save substantial effort in post-processing the data.
- MicMac, the third module, starts from the optimal orientations calculated by Apero. It consists in producing an accurate and dense depth map of the scene. A depth map contains distance information of all points of the scene that are seen from a viewpoint. It can be converted

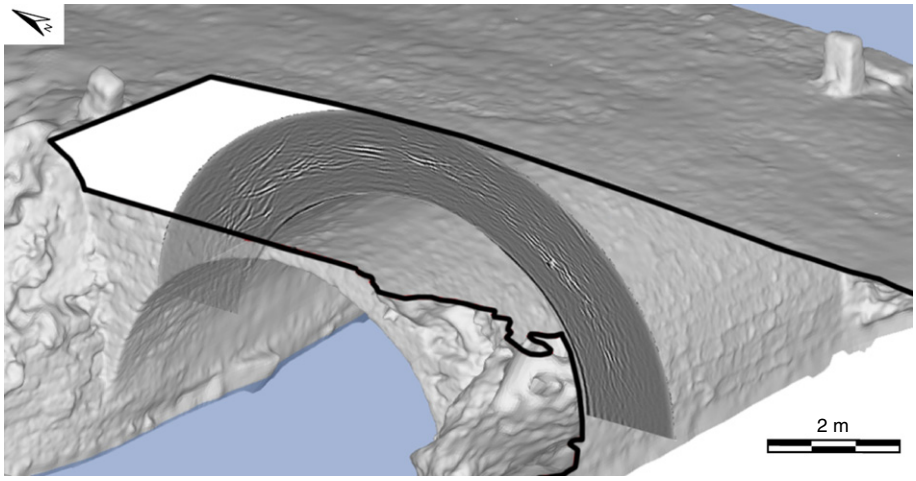

Fig. 16. Digital Terrain Model of the bridge with a radial GPR profile on the arch barrel.

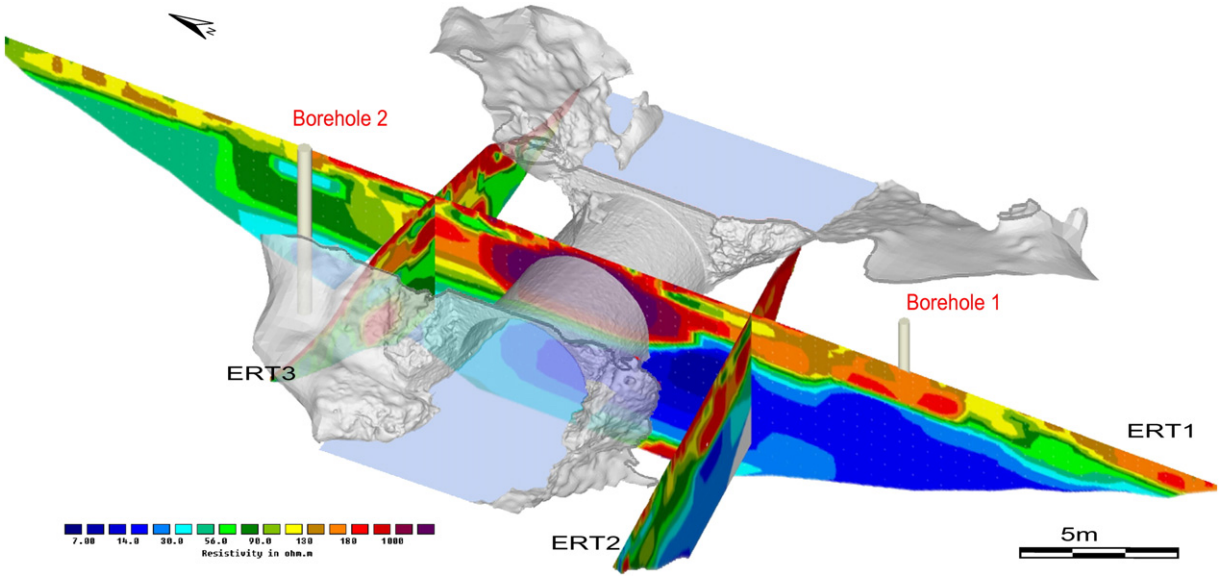

Fig. 17. Digital Terrain Model of the bridge with superimposed ERT profiles and boreholes.

into a 3D point cloud, which is generated by means of an energy minimization algorithm. The cost function is the sum of two terms: one that accounts for the correlation between areas of the images and the other that accounts for the smoothness of the reconstructed 3D surface (local gradient). The minimization problem is solved by a multiscale dynamic programming algorithm, with a pyramidal structure for the computation. This algorithm takes advantage of the redundancy of the images (each point is actually seen by 10 images). MicMac computes the DTM in a Euclidean space, so the result is a grid where $z = f(x,y)$. It is well adapted to flat scenes and has the advantage of storing the result in a single depth map.

Apero-MicMac is more complex to use compared to other open source software but, in return, it is more complete and accurate. Protocols for architectural studies are described in (Pierrot Deseilligny and Clery, 2011, 2012). However, this method has never been adapted in order to highlight a geophysical study. A first attempt is described in the following.

A set of images of the bridge and its surroundings were taken in June 2012. The acquisition protocol was very simple: the photos have been captured by hand around the bridge (at a maximum distance of 10 m) and under its vault (at a maximum distance of ≈1.50 m), with a Panasonic GF1 camera (focal of 28 mm). In this case, the size of the images is 12 Megapixels and the size of the sensor is 18 × 13.5 mm. The set of images must cover the entire scene and each part of the landscape must appear on at least 2 photos, taken with different angles of view. A total amount of 150 images have been acquired, capturing the whole scene and details of the bridge. Under the arch, an image was taken with a metric step to cover the structure with a maximum overlap. Finally, a maximum overlap of 90 percents was obtained between the different photos (Fig. 13).

Once acquired, the set of images serves as input data for the first module and Apero. This process allows to search for tie-points and to compute the relative orientation of the images (Fig. 14). The last step corresponds to the production of a dense depth map of the scene by the MicMac module, starting from the optimal orientations calculated by Apero (Fig. 15).

The final DTM of the Pont de Coq contains a total of 3.5 millions points and its length is nearly 50 m. Then, the resolution of the model is ≈2 cm (Fig. 15).

Once the high resolution 3D point cloud is obtained, a surface model is computed with the Meshlab™ software using a Poisson's reconstruction. Then, the result is included within a CAD software to integrate any available data. In this study, we used the free Google Sketchup™ software to integrate the GPR and ERT data in the model (Figs. 16 and 17). Such model is an easy to use tool for the stakeholder who is unused of geophysical methods: it allows a better representation of the bridge and its geophysical characteristics. Finally, it leads to an improved interpretation of the available data for a better assessment of the structure.

7. Discussion

The 400 MHz and 1.5 GHz GPR measurements allowed a qualitative assessment of the internal structure of the bridge. The profiles carried out on the deck and on the arch barrel yielded the detection of roots and defects that can be voids or weathered zones behind the stones (paved surface or voussoirs) and/or inside the backfill material. Our sampling space was 50 cm. A thinner space sampling could have been applied for the deck survey and the arch barrel in order to obtain a more detailed investigation. Moreover, the use of 1.5 GHz antenna providing approximately a vertical resolution of 4 cm could have been used on the deck to enhance the results. In such case a 3D volume estimation of anomalies within the backfill would have been possible using migration methods and 3D processing of the GPR profiles. Nevertheless, the detection of roots inside the backfill, behind the voussoirs at various depths is well achieved with radial 1.5 GHz GPR survey.

The use of the ERT method provides an interpreted imaging of the material distribution inside the riverbanks, under the roadway and inside the bridge abutments. It gives precious information about the local geology. The ERT allowed us to extend our study at a large scale using two boreholes logs. One of the main results of ERT survey is the detection of the clayey layer beneath the road and the bridge. This result yields the conclusion that the bridge can be anchored inside this clay layer with wooden piles (a common civil engineering method before being replaced by concrete piles). This ERT interpretation is improved by the 200 MHz GPR survey and strong correlations are achieved in terms of materials identification and location. The GPR is recommended for structures composed of resistive materials such as the road and the bridge. It provides an image of the internal structure with a high spatial resolution. The ERT method provides information for both conductive and resistive materials. However, the results are non-unique due to the inversion processing and highly dependent on the acquisition configuration. In our case, the ERT survey allowed us to clearly distinguish the man-made materials from the alluvial deposits.

The photogrammetry is a valuable method for the 3D visualization of geophysical results. The images were acquired with an experimental approach that is not fully optimized. Improvements in the acquisition protocol (using of wide angle focal and a defined location of the camera) will facilitate the processing of the photogrammetric data. The present high resolution results are encouraging and offer a powerful, cost-effective and free tool for advanced geophysical imaging and analysis.

8. Conclusion

We performed an original study combining geotechnical data, geophysical and photogrammetric observations. Several GPR profiles carried out on the bridge (deck and arch barrel) revealed the presence of roots and potential voids in the structure. It is obvious that the strongest GPR reflections indicate suspicious defects able to threat the mechanical stability of the bridge. They should be destructively controlled to be interpreted. Nevertheless, the abutments, the arch barrel and the deck of the bridge remain in relatively good condition.

The combination of the GPR and ERT methods yields the characterization of the surrounding subsurface. The geophysical data are well correlated with the sedimentological data provided by borehole logging. Both methods allow the description of the geology at a local scale. The road is built on a man-made silty backfill overlaying the Middle Portlandian clayey substratum. The driven wooden piles under the bridge abutments are anchored in this clay formation. This configuration has allowed the bridge to survive hundreds of years of drop. The photogrammetry method led to the making of a DEM of the bridge with a centimetric resolution. It offers to the stakeholder a powerful tool for the 3D visualization of the potential defects present within the bridge.

This study was led for historical preservation purposes. Once again, it shows the ability of non destructive methods (GPR and ERT) for assessing the civil engineering buildings. Moreover, new perspectives are now highlighted with the addition of the photogrammetry method, providing a high quality restitution of the measurements in the field. More generally, such approach may ease the realization of high resolution 3D geophysical and geological models for geoscience purposes.

Acknowledgment

We are very grateful to the CETE — Normandie Centre and the University of Rouen (M2C and ECODIV) who supported these measurements and to the following persons for their contribution during the survey: Bruno Beaucamp, Vincent Guilbert, Cyril Ledun and Carole Kaouane of the ERA23 crew.

References

Arias, P., Armesto, J., Di-Capua, D., González-Drigo, R., Lorenzo, H., Pérez-Gracia, V., 2007. Digital photogrammetry, GPR and computational analysis of structural damages in a mediaeval bridge. Eng. Fail. Anal. 14, 1444–1457.

Blondeau, A., Fraisse, C., Pomerol, B., Pomerol, C., 1979. Carte géologique de forges-les-eaux au 1:50 000ème et sa notice explicative, 26. BRGM, Orléans.

Boothby, T., Rusnak, C., Hawkins, J., Elefteriadou, A., 1998. Stone Arch Bridge Inventory, Phase II. Technical Report.The Pennsylvania State University, University Park, PA 16802.

Bretar, F., Arab-Sedze, M., Champion, J., Pierrot-Deseilligny, M., Heggy, E., Jacquemoud, S., 2013. An advanced photogrammetric method to measure surface roughness: application to volcanic terrains in the Piton de la Fournaise, Reunion Island. Remote. Sens. Environ. 135, 1–11.

Chandler, J.H., Fryer, J.G., Jack, A., 2005. Metric capabilities of low-cost digital cameras for close range surface measurement. Photogramm. Rec. 20, 12–26.

Colla, C., Das, P.C., McCann, D., Forde, M.C., 1997. Sonic, electromagnetic and impulse radar investigation of stone masonry bridges. NDT E Int. 30, 249–254.

Doetsch, J., Linde, N., Pessognelli, M., Green, A.G., Günther, T., 2012. Constraining 3-d electrical resistance tomography with gpr reflection data for improved aquifer characterization. J. Appl. Geophys. 78, 68–76.

Ercoli, M., Pauselli, C., Forte, E., Di Matteo, L., Mazzocca, M., Frigeri, A., Federico, C., 2012. A multidisciplinary geological and geophysical approach to define structural and hydrogeological implications of the Molinaccio Spring (Spello, Italy). J. Appl. Geophys. 77, 72–82.

Flint, R.C., Jackson, P.D., McCann, D.M., 1999. Geophysical imaging inside masonry structures. NDT E Int. 32, 469–479.

Gourry, J.C., Vermeersch, F., Garcin, M., Giot, D., 2003. Contribution of geophysics to the study of alluvial deposits: a case study in the Val d'Avaray area of the River Loire, France. J. Appl. Geophys. 54, 35–49.

Hing, C., Halabe, U., 2010. Nondestructive testing of GFRP bridge decks using ground penetrating radar and infrared thermography. J. Bridg. Eng. 15, 391–398.

Hugenschmidt, J., Mastrangelo, R., 2006. Gpr inspection of concrete bridges. Cem. Concr. Compos. 28, 384–392.

Locke, M., 2012. Tutorial: 2-D and 3-D electrical imaging surveys. Copyright (1996–2011) M.H.Loke.

Loke, M., Barker, R., 1996. Rapid least-squares inversion of apparent resistivity pseudosections by a quasi-newton method1. Geophys. Prospect. 44, 131–152.

Lowe, D., 2004. Distinctive image features from scale-invariant keypoints. , 60 91–110.

Lubowiecka, I., Arias, P., Riveiro, B., Solla, M., 2011. Multidisciplinary approach to the assessment of historic structures based on the case of a masonry bridge in Galicia (Spain). Comput. Struct. 89, 1615–1627.

Maisonnave, C., 2012. Etude géologique des abords du pont de coq (haute-normandie). ASPC report, 32.

McCann, D.M., Forde, M.C., 2001. Review of NDT methods in the assessment of concrete and masonry structures. NDT E Int. 34, 71–84.

Nuzzo, L., Calia, A., Liberatore, D., Masini, N., Rizzo, E., 2010. Integration of ground-penetrating radar, ultrasonic tests and infrared thermography for the analysis of a precious medieval rose window. Adv. Geosci. 24, 69–82.

Orbán, Z., Gutermann, M., 2009. Assessment of masonry arch railway bridges using non-destructive in-situ testing methods. Eng. Struct. 31, 2287–2298.

Orbán, Z., Yakovlev, G., Pervushin, G., 2008. Non-destructive testing of masonry arch bridges — an overview. Bautechnik 85, 711–717.

Pierrot Deseilligny, M., Clery, I., 2011. Apero, an open source bundle adjustment software for automatic calibration and orientation of set of images. Int. Arch. Photogramm. Remote. Sens. Spat. Inf. Sci. XXXVIII-5 (W16), 269–276.

Pierrot Deseilligny, M., Clery, I., 2012. Some possible protocols of acquisition for the optimal use of the äpero" open source software in automatic orientation and calibration. Tutorial for EuroCow, Castelldefels, Espagne, 8–10 February 2012.

Ranalli, D., Scozzafava, M., Tallini, M., 2004. Ground penetrating radar investigations for the restoration of historic buildings: the case study of the collemaggio basilica (L'Aquila, Italy). J. Cult. Herit. 5, 91–99.

Sandmeier, K., 2004. ReflexW version 3.5. Program for processing of seismic, acoustic and electromagnetic reflection, refraction and transmission data. Software manual.Karlsruhe, Germany (345 pp.).

Solla, M., Lorenzo, H., Novo, A., Rial, F., 2010. Ground-penetrating radar assessment of the medieval arch bridge of San Antón, Galicia, Spain. Archaeol. Prospect. 17, 223–232.

Solla, M., Lorenzo, H., Novo, A., Riveiro, B., 2011a. Evaluation of ancient structures by GPR (ground penetrating radar): the arch bridges of Galicia (Spain). Sci. Res. Essays 8, 1877–1884.

Solla, M., Lorenzo, H., Rial, F.I., Novo, A., 2011b. GPR evaluation of the roman masonry arch bridge of Lugo (Spain). NDT E Int. 44, 8–12.

Solla, M., Caamaño, J.C., Riveiro, B., Arias, P., 2012. A novel methodology for the structural assessment of stone arches based on geometric data by integration of photogrammetry and ground-penetrating radar. Eng. Struct. 35, 296–306.